

This document is confidential and is proprietary to the American Chemical Society and its authors. Do not copy or disclose without written permission. If you have received this item in error, notify the sender and delete all copies.

INCORPORATING FOULING MODELING INTO SHELL-AND-TUBE HEAT EXCHANGER DESIGN

Journal:	<i>Industrial & Engineering Chemistry Research</i>
Manuscript ID	ie-2016-03564a
Manuscript Type:	Article
Date Submitted by the Author:	14-Sep-2016
Complete List of Authors:	Nakao, Andressa; Universidade Federal do Rio de Janeiro Valdman, Andrea; Universidade Federal do Rio de Janeiro Costa, André; Rio de Janeiro State University (UERJ), Bagajewicz, Miguel; University of Oklahoma, School of Chemical Engineering and Materials Science Queiroz, Eduardo; Universidade Federal do Rio de Janeiro

SCHOLARONE™
Manuscripts

INCORPORATING FOULING MODELING INTO SHELL-AND-TUBE HEAT EXCHANGER DESIGN

*Andressa Nakao,[†] Andrea Valdman,[†] André L. H. Costa,[‡] Miguel J. Bagajewicz,⁺ Eduardo M.
Queiroz^{*†}*

[†] Federal University of Rio de Janeiro (UFRJ), Escola de Química CT, Bloco E, Ilha do Fundão,
CEP 21949-900, Rio de Janeiro, RJ, Brazil, mach@eq.ufrj.br

[‡] Institute of Chemistry, Rio de Janeiro State University (UERJ), Rua São Francisco Xavier, 524,
Maracanã, Rio de Janeiro, RJ, CEP 20550-900, Brazil.

⁺ School of Chemical, Biological and Materials Engineering, University of Oklahoma, Norman,
Oklahoma USA 73019.

^{*}Corresponding author.

ABSTRACT

Fouling is a major problem in the operation of heat exchangers, resulting in increased capital, operational and maintenance costs. Shell-and-tube heat exchangers are normally designed using fixed values of fouling resistances, ignoring that fouling rates depend on the exchanger geometry, rendering different fouling resistances for the same thermal service. This article discusses the use of fouling rate models in the design of shell-and-tube heat exchanger. We link a heat exchanger design algorithm to a dynamic simulation of the fouling rate. Three examples illustrate how the utilization of the fouling rate model alters the solution of the design problem. Also, aspects related to a “no fouling” condition in the design and the impact of the duration of the operational campaign in the results are also analyzed.

1. INTRODUCTION

Due to the structural simplicity, flexibility and robustness, shell-and-tube heat exchangers are the most common heat transfer alternative used in power plants, oil refineries, and chemical plants.

The shell-and-tube heat exchanger design problem includes several interdependent qualitative and quantitative elements. Traditionally, it is a procedure strongly based on the designer experience. Nowadays, there are several commercial software available to assist heat exchanger designers, such as HTRI and Aspen Shell and Tube Exchanger. These tools contain algorithmic routines that may provide automatic solutions for the heat exchanger design problem.¹ Additionally, the literature contains a considerable number of papers that employs optimization tools for the solution of the design problem. These procedures involve a diversity of approaches, encompassing a variety of objective functions, design variables and optimization methods. The solution techniques investigated include mathematical programming,²⁻⁴ stochastic methods,⁵⁻⁶ algorithmic screenings of a counting table,⁷ etc.

However, independently of the approach, the fouling problem is usually considered in the design using fixed fouling factors, which estimate the impact of the deposits in the heat exchanger performance. Despite the development of fouling rate models, the utilization of model predictions in the design is relatively scarce in the literature: Butterworth⁸ explored the utilization of the fouling rate in the heat exchanger design through three approaches: (a) searching for the design associated to a “no fouling” conditions; (b) design the heat exchanger using an asymptotic value of the fouling resistance based on a rate model; and (c) explore the fouling rate in the design according to an assumed operational history. The design analysis is

1
2
3 conducted based on a graphical representation of the feasible solutions in relation to the number
4 and length of the tubes. The same graph was also employed by Wilson et al.⁹ to analyze how
5 different alternatives of shell and tube heat exchangers are affected by fouling in the design.
6
7
8
9
10 Nesta and Bennet¹⁰ presented guidelines to be employed in the design of a heat exchanger to
11 suppress fouling. Finally, Caputo et al.¹¹ presented a heat exchanger design method, where the
12 exchanger optimization is made with maintenance considerations. In their approach, the authors
13 include the cleaning schedules cost in the final cost and define a maximum allowable fouling
14 resistance during the operating time. Empirical fouling rate models, dependent on the flow
15 velocity, are employed for estimating the fouling resistance values during the period between
16 cleaning shutdowns.
17
18
19
20
21
22
23
24
25
26

27
28 Aiming at contributing to this effort of inserting the fouling phenomenon in the design beyond
29 the conventional fixed fouling resistances, this paper presents a design procedure where the
30 fouling resistance is calculated based on the thermofluidynamic conditions of the design itself.
31
32 This interrelation is provided by coupling the design algorithm to a dynamic simulation (pseudo-
33 stationary) of the heat exchanger subjected to fouling. The convergence between the fouling
34 resistance used in the design and the final fouling resistance in the simulation is promoted by a
35 convergence loop. Among the different fouling problems, this paper presents the proposed
36 procedure applied to chemical reaction fouling in crude oil streams.
37
38
39
40
41
42
43
44
45
46

47
48 The article is organized as follows. Section 2 describes the fouling modelling associated to the
49 design, Section 3 presents the heat exchanger simulation using the fouling rate model, Section 4
50 presents the proposed procedure of interconnection between the design algorithm and the fouling
51 rate model, Section 5 explores the proposed procedure through three examples, and Section 6
52 presents the Conclusions.
53
54
55
56
57
58
59
60

2. FOULING MODELING

In heat transfer technology, fouling is the undesired accumulation of deposits over the thermal surface of heat exchanger equipment. It causes an increase of capital, operating and maintenance costs. Its usage in heat exchanger design is based on the insertion of additional resistances in the thermal circuit between the hot and cold streams. The overall heat transfer coefficient in the design considering the presence of fouling (U_{dirty}) encompasses the convective heat transfer resistances, the wall conductive resistance and the resistances associated to fouling and is given by:

$$U_{dirty} = \frac{1}{\frac{1}{ht} \left(\frac{dte}{dti} \right) + Rft \left(\frac{dte}{dti} \right) + \frac{dte \ln(dte/dti)}{2ktube} + Rfs + \frac{1}{hs}} \quad (1)$$

where ht and hs are the convective heat transfer coefficients in the tube-side and shell-side, dte and dti are the outer and inner tube diameters, $ktube$ is the thermal conductivity of the tube wall, and Rft and Rfs are the fouling resistances associated to the tube-side and shell-side streams.

This expression can be related to the overall heat transfer condition in the clean condition (U_{clean}):

$$U_{dirty} = \frac{1}{\frac{1}{U_{clean}} + Rf} \quad (2)$$

where Rf encompasses the fouling resistances of both streams.

Fouling resistances imply a higher heat transfer area needed in the design to guarantee that the heat exchanger will attain the needed heat load according to the process specifications during the entire period between cleaning shutdowns. If the fouling resistance presents an asymptotic

1
2
3 behavior, the adequate insertion of the fouling resistance would allow the continuous operation
4 of the heat exchanger without cleaning. Typical values of fouling resistances can be found in
5 tables available in the literature. Usually, in these tables, the values of the fouling resistance are
6 only associated to the nature of the stream for the majority of the fluids. In more specific tables
7 (e.g. TEMA), for some specific fluids (e.g. water and crude oil), the fouling resistance values are
8 associated to ranges of flow velocity and fluid temperature.
9

10
11
12
13
14
15
16
17
18
19 The central idea of the current paper is to employ fouling rate models to determine the fouling
20 resistance to be employed in the design. The fouling rate model employed must be able to
21 describe the impact of the thermofluidynamic conditions on fouling for each design alternative
22 (e.g. two design solutions associated to distinct values of flow velocities must present different
23 values of fouling resistances for the same service).
24
25
26
27
28
29

30
31 The first rate model describing fouling behavior was developed by Kern and Seaton in 1959.¹²
32
33 The model considers fouling as a result of two simultaneous processes: a deposition process and
34 a removal process:
35
36
37

$$\frac{dR_f}{dt} = \varphi_D - \varphi_R \quad (3)$$

38
39
40
41
42 where φ_D and φ_R are the deposition and removal rates, respectively.
43
44

45
46 Because of fouling may be associated to different causes (sedimentation, precipitation,
47 chemical reaction, biological growth, corrosion, and freezing), the phenomenological
48 determination of the deposition and removal rates depends on the specific nature of the stream
49 flowing in the heat exchanger. In this context, the present design procedure can be employed
50 using any fouling rate model dependent on the thermofluidynamic conditions. Particularly, the
51
52
53
54
55
56
57
58
59
60

analysis presented here is focused on crude oil fouling associated to the presence of asphaltenes (chemical reaction fouling).

There are three approaches for fouling rate models in crude oil streams: (i) deterministic; (ii) semi-empirical; and (iii) artificial neural network.¹³ In the deterministic approach, some researchers have presented fouling rate models based on physical analysis, similar to particulate and crystallization fouling studies, but due to the complexity of the crude oil nature, these models lost importance. The semi-empirical approach includes the effects of the operational variables (e.g. flow velocity and film/wall temperature) for the fouling rate description, where the model parameters must be determined through parameter estimation procedures using experimental or plant data. The last approach incorporates statistical learning algorithms creating relationships between different variables related to fouling phenomenon.

Among the existent alternatives, semi-empirical models using the threshold fouling concept of Ebert and Panchal assume a central role in the literature.¹⁴ The Ebert and Panchal model describes fouling as a phenomenon controlled by two mechanisms that compete between themselves: deposition and suppression, indicating the possibility of a “no fouling condition” where these two mechanisms cancel each other out.¹⁵ This concept is the base of several later similar models.¹⁶⁻¹⁸

Among the different alternatives, it is used in this paper the Ebert-Panchal modified fouling rate model,¹⁶ with the suggestion of Lestina and Zettler¹⁹ to employ the surface temperature instead of the film temperature:

$$\frac{dR_f}{dt} = \alpha Re^{-0.66} Pr^{-0.33} \exp\left(-\frac{E_a}{RT_{surf}}\right) - \gamma \tau_w \quad (4)$$

1
2
3 where Re and Pr represent the Reynolds and the Prandtl numbers, R is the universal gas constant,
4
5 T_{surf} is the fouling surface temperature, τ_w is the shear stress, α and γ are empirical model
6
7 parameters which, together with the fouling activation energy (E_a), must be estimated based on
8
9 experimental or plant data. The shear stress can be calculated by:
10
11

$$\tau_w = f\rho \frac{v^2}{2} \quad (5)$$

12
13
14 where f is the Fanning friction factor, ρ is the specific mass, and v is the mean flow velocity. The
15
16
17 friction factor expression can be given by:²⁰
18
19
20
21

$$f = 0.0035 + \frac{0.264}{Re^{0.42}} \quad (6)$$

22
23
24
25
26 The first term in the RHS of Eq. 4 corresponds to the deposition and the second term
27
28 represents suppression. The interpretation of the negative term as a suppression effect instead of
29
30 the traditional Kern and Seaton's removal is still object of discussion in the literature.^{13,21}
31
32

33
34 Using the fouling rate equation, the threshold concept can be graphically described by a
35
36 fouling envelope, as it is illustrated in Figure 1. This envelope allows the observation of fouling
37
38 and no fouling regions.
39
40
41
42
43
44
45
46
47
48
49
50
51
52
53
54
55
56
57
58
59
60

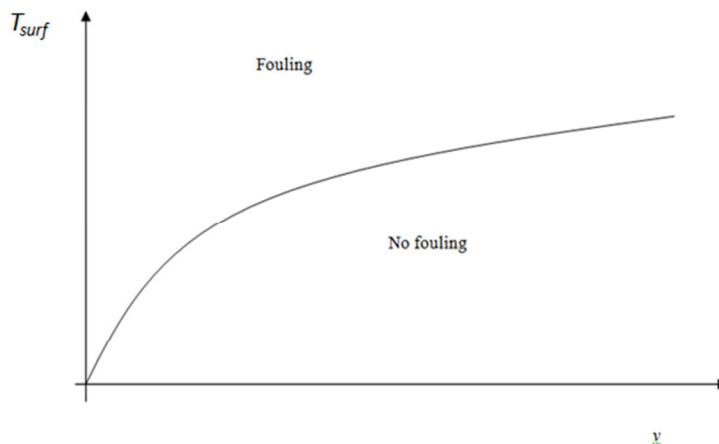


Figure 1. Representation of the threshold concept in relation to the surface temperature (T_{surf}) and the flow velocity (v).

3. HEAT EXCHANGER SIMULATION

The analysis of the heat exchanger behavior affected by fouling associated to the design algorithm involves its simulation during the period between cleaning shutdowns. Since fouling is a slow process, the dynamic simulation of the heat exchanger can be done using a pseudo-stationary model. The resultant mathematical model is composed of the fouling rate differential equation together with algebraic equations of the steady-state model using the ε -NTU method and an equation for evaluation of the fouling surface temperature. The reduction of the inner diameter due to the fouling thickness growth is not considered in the model.

3.1. Fouling rate. According to the previous section, the fouling rate model employed is the modified Ebert-Panchal model, where fouling occurs in the tube-side due to the crude oil heating (the fouling in the shell-side is considered null). Along the heat exchanger area, the stream temperature profiles imply that each point of the heat exchanger presents a different fouling rate.

Aiming to avoid a more complex model (which would involve partial differential equations), the spatial variation of the fouling rate is substituted by an average value calculated using the fouling rates at the heat exchanger ends in an equivalent countercurrent configuration:

$$\left(\frac{dR_f}{dt}\right)_{avg} = \frac{1}{2} \left[\left(\frac{dR_f}{dt}\right)_1 + \left(\frac{dR_f}{dt}\right)_2 \right] \quad (7)$$

where the subscripts 1 and 2 indicate the heat exchanger ends. A more accurate alternative that could be also employed for the determination of the average fouling rate is described in Ishiyama et al.²²

Adopting the suppression hypothesis, the fouling rate will never assume negative values, i.e., it is considered that the shear stress would not be able to remove any existent deposits. Therefore, the final form of the fouling rate model becomes:

$$\frac{dR_f}{dt} = \max\left(0, \left(\frac{dR_f}{dt}\right)_{avg}\right) \quad (8)$$

3.2. Steady-State Heat Exchanger Equations. The heat exchanger model employs the ε -NTU method.²³ This method contains three dimensionless variables: the effectiveness (ε), the number of transfer units (NTU), and the ratio between heat capacity flow rates (C_R):

$$\varepsilon = \frac{Q}{Q_{max}} \quad (9)$$

$$NTU = \frac{U_{foul}A}{C_{min}} \quad (10)$$

$$C_R = \frac{C_{min}}{C_{max}} \quad (11)$$

where Q is the heat load, Q_{max} is the maximum heat load thermodynamically possible, U_{foul} is the fouled overall heat transfer coefficient at a given moment, A is the heat transfer area, C_{min} and

1
2
3 C_{max} are the heat capacity flow rates (mCp) of the minimum and maximum fluids (respectively,
4 the streams with the higher and lower heat capacity flow rates). The fouled overall heat transfer
5 coefficient is calculated using the value of the fouling resistance at the respective instant of the
6 integration path.
7
8
9
10

11
12
13
14 The thermodynamic limit of the heat load is given by:

$$15 \quad Q_{max} = C_{min}(T_{h,i} - T_{c,i}) \quad (12)$$

16
17
18 where $T_{h,i}$ and $T_{c,i}$ are the inlet temperatures of the hot and cold streams, respectively.
19
20
21
22

23 Using energy balances and the heat transfer rate equation, it is possible to establish a relation
24 among these three variables:
25
26
27

$$28 \quad \varepsilon = \varepsilon(NTU, C_R) \quad (13)$$

29
30
31 The ε -NTU relations are available for each specific heat exchanger configuration. For
32 example, the ε -NTU relation for a heat exchanger with a countercurrent configuration is:
33
34
35
36
37

$$38 \quad \varepsilon = \frac{1 - \exp[-NTU(1 - C_R)]}{1 - C_R \exp[-NTU(1 - C_R)]} \quad (14)$$

39
40
41 The outlet temperatures of the heat exchanger can be evaluated from the effectiveness. The
42 corresponding equations are represented below, when the minimum fluid is the hot stream (as
43 occur in crude preheat trains):
44
45
46
47
48

$$49 \quad T_{h,o} = T_{h,i} - \frac{\varepsilon Q_{max}}{C_{min}} \quad (15)$$

$$50 \quad T_{c,o} = T_{c,i} + \frac{\varepsilon Q_{max}}{C_{max}} \quad (16)$$

51
52
53
54
55
56 Equivalent equations can be deducted when the cold stream is the minimum fluid.
57
58
59
60

1
2
3 **3.3. Surface Temperature Equation.** The temperature of the surface in contact with the cold
4 stream can be calculated through the thermal circuit between hot and cold streams:
5
6
7

$$\frac{T_h - T_{surf}}{\frac{1}{h_s D_{te}} + \frac{\log(D_{te}/D_{ti})}{2k_{tube}} + \frac{R_f}{D_{ti}}} = \frac{T_{surf} - T_c}{\frac{1}{h_t D_{ti}}} \quad (17)$$

12 13 14 15 16 **4. EXCHANGER DESIGN AND FOULING RATE MODELING**

17
18
19 The proposed procedure is composed of two main steps: the design algorithm and the heat
20 exchanger simulation. This analysis can employ any heat exchanger design algorithm available,
21 where it is illustrated here the utilization of the design option of the HTRI software.
22
23
24

25
26
27 Firstly, the HTRI design tool is used to obtain a shell-and-tube heat exchanger design
28 candidate for the required service based on an estimated fouling resistance (e.g. TEMA value).
29 To run this step, a set of parameters must be defined by the engineer: fluid allocation (tube or
30 shell), materials (shell, tube, etc.), shell and heads types, baffle type and cut, tube pitch ratio,
31 tube layout pattern, outer tube diameter and tube wall thickness. The searched parameters by the
32 software in the design are: inner shell diameter, total number of tubes, number of tubes passes,
33 tube length and baffle spacing.
34
35
36
37
38
39
40
41
42
43
44

45 After the design made by HTRI, the corresponding heat exchanger is simulated for the planned
46 operational run between cleaning shutdowns. The convective heat transfer coefficients employed
47 in the simulation are extracted from the HTRI run, therefore guaranteeing the accuracy of the
48 results.
49
50
51
52
53
54
55
56
57
58
59
60

1
2
3 The final value of the fouling resistance is then compared with the initial estimate (see Figure
4
5
6 2). If the values are similar according to a certain tolerance, the procedure is finished, otherwise
7
8 the HTRI is executed again with the new value of the fouling resistance. The steps are repeated
9
10 until convergence is achieved.
11

12
13
14 Computational tests have indicated that sometimes convergence is not reached, therefore
15
16 another stopping criterion is included in the algorithm based on the maximum number of
17
18 iterations. The analysis of the results of the search in the non-converged cases indicates a cyclic
19
20 repetition of a sequence of fouling resistances. In these cases, the design solution corresponds to
21
22 the alternative associated to the smallest value of input fouling resistance, which yields in the
23
24 dynamic simulation a lower final fouling resistance, i.e. the solution presents a design fouling
25
26 resistance higher than the maximum value reached during the simulation, thus guaranteeing a
27
28 feasible design according to the fouling rate model.
29
30
31

32
33
34 The convergence scheme runs automatically in a Matlab environment. The code includes
35
36 subroutines for the communication between Matlab and HTRI, and subroutines to solve the
37
38 differential-algebraic system of equations, using the DASSL solver.
39
40
41
42
43
44
45
46
47
48
49
50
51
52
53
54
55
56
57
58
59
60

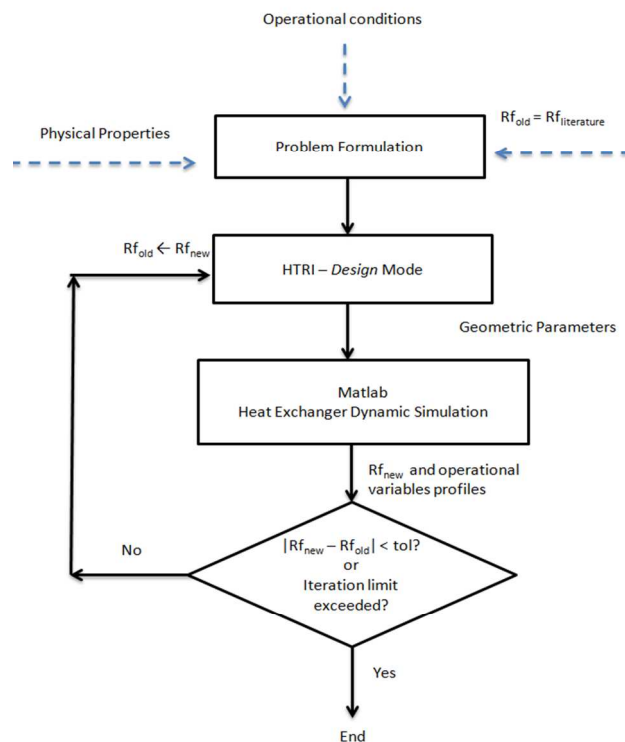


Figure 2. Design procedure using fouling rate modelling.

5. EXAMPLES

In order to show the performance of the proposed procedure, three examples are investigated, representing crude preheat train exchangers without phase change. These examples represent the same design task, but involving different sets of fouling rate parameters. The basic specifications of the heat exchanger design is depicted in Table 1, the search space is described in Table 2 and the data of the streams are shown in Table 3. The dynamic simulations are conducted considering a two years period between cleanings for the Examples 1 and 2. Example 3 analyzes operation campaigns with different durations, aiming to investigate the impact of the cleaning frequency in the design. The initial value of the fouling resistance adopted in the search is based on the TEMA

value, consistent with the crude heating design task: dry crude, velocity higher than 4 ft/s and temperature range between 250 °F and 350 °F.²⁴

Table 1. Basic Specifications of the Heat Exchangers

	Specification
TEMA type	AES
baffle type	single segmental
baffle cut (%)	25
tube pitch ratio	1.25
tube layout	triangular
outer tube diameter (mm)	19.05
tube thickness (mm)	2.1

Table 2. Input Specifications in the HTRI Design Mode

	Specification
number of tube passes	1, 2, 4, 6, ...
tube length	4.0 , 4.5 , 5.0 , 5.5 , 6.0
overdesign (%)	0 to 10
tube side velocity bounds (m/s)	1.0 to 3.0
shellside velocity bounds (m/s)	0.5 to 2.0

Table 3. Example 1 - Specifications of the Streams

	Hot stream	Cold stream
mass flow rate (kg/s)	45.0	95.0
inlet temperature (°C)	255	165
outlet temperature (°C)	229	180
specific mass (kg/m ³)	852	819
heat capacity (kJ/kg·K)	2.9	2.4
viscosity (Pa·s)	1.7·10 ⁻³	1.3·10 ⁻³
thermal conductivity (W/m·K)	0.11	0.10
allowable pressure drop (kPa)	70	70

5.1. Example 1. The fouling rate model parameters (Eq. (4)) are shown in Table 4, coherent with the range displayed in Wilson et al..¹³

Table 4. Example 1-Fouling Rate Model Parameters (Eq. (4))

	Parameter
α (m ² K/J)	1.078
E_a (kJ/mol)	40
γ (m ² K/J·Pa)	$4.03 \cdot 10^{-11}$

The application of the proposed procedure obtained a solution after four iterations. Table 5 presents the design solution found (final design) and Table 6 displays the corresponding thermofluidynamic variables. These tables also depict the initial heat exchanger designed using the TEMA fouling factor (initial design). The design fouling resistance presented in Table 5 corresponds to the value employed in the HTRI input and the simulated fouling resistance is the corresponding value at the end of the simulation.

The comparison between both solutions indicates that the proposed procedure was able to modify the initial design according to the fouling rate model predictions. The equivalence of the design and simulated fouling resistances in the final design shows the convergence of the algorithm, according to the tolerance selected.

Starting from the TEMA fouling resistance value, the algorithm identifies a heat exchanger with an area 18.3% smaller, based on the fouling rate model attached to the design algorithm.

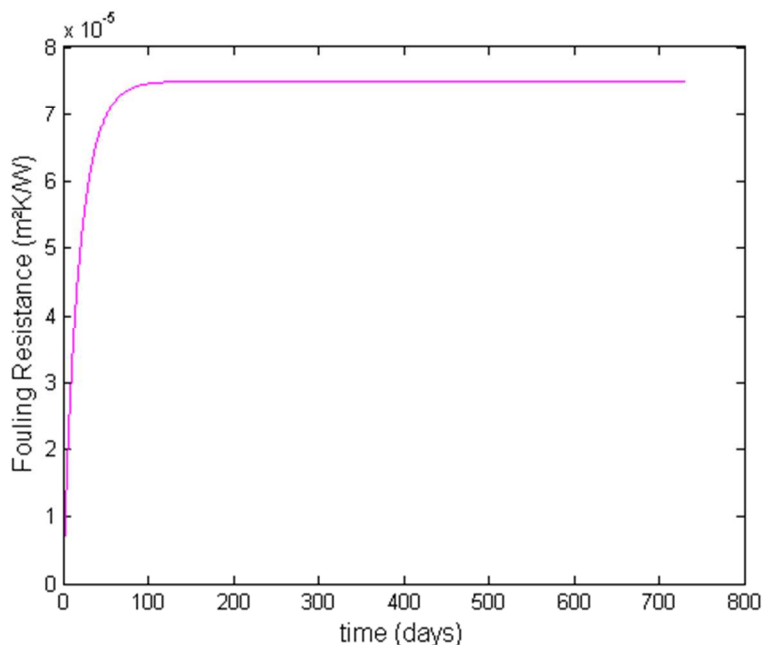
Table 5. Example 1 - Heat Exchanger Design Solutions: Design Variables

	initial design	final design
design fouling resistance (m ² K/W)	0.000350	0.0000750
simulated fouling factor (m ² K/W)	0.00113	0.0000749
area (m ²)	76.76	62.70
total number of tubes	235	235
number of tube passes	1	1
shell diameter (m)	0.438	0.438
tube length (m)	5.5	4.5
baffle spacing (m)	0.394	0.370

Table 6. Example 1 - Heat Exchanger Design Solutions: Thermofluidynamic Variables

	initial design	final design
Overall heat transfer coefficient ($\text{W}/\text{m}^2\text{°C}$)	660.7	865.7
tube-side film coefficient ($\text{W}/\text{m}^2\text{°C}$)	2340.3	2359.3
shell-side film coefficient ($\text{W}/\text{m}^2\text{°C}$)	2118.8	2123.7
tube-side flow velocity (m/s)	2.86	2.86
shell-side flow velocity (m/s)	0.96	1.00
tube-side pressure drop (kPa)	43.9	37.5
shell-side pressure drop (kPa)	66.0	58.6

Profiles of the simulation of the final design solution are presented in Figures 3, 4 and 5. These figures show a continuous increase of the fouling resistance associated to the corresponding modification of the outlet temperatures. It is important to observe that the values of the temperatures determine a heat load during the entire period higher than the service specification.

**Figure 3.** Fouling resistance profile of Example 1

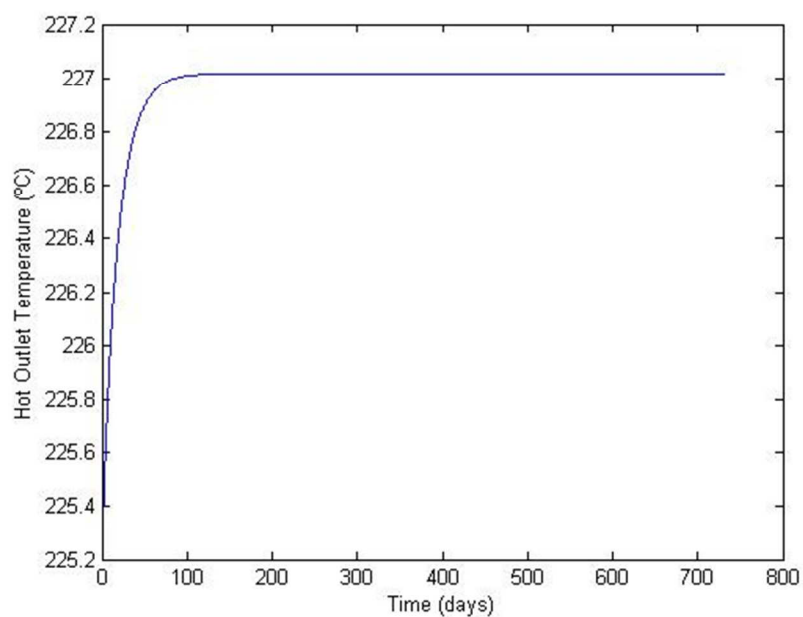


Figure 4. Outlet temperature of the hot stream in Example 1

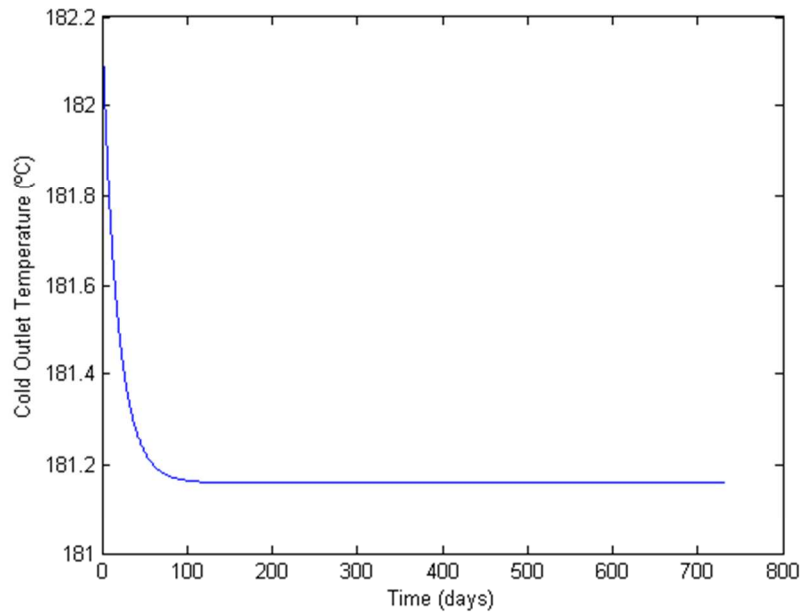


Figure 5. Outlet temperature of the cold stream in Example 1

5.2. Example 2. The fouling rate model parameters are displayed in Table 7. The basic specifications of the design are the same of the previous example.

Table 7. Example 2 -Fouling Rate Model Parameters (Eq. (4))

	Parameter
α (m ² K/J)	13.97
E_a (kJ/mol)	48
γ (m ² K/J·Pa)	$3.44 \cdot 10^{-8}$

The initial and final design solutions with thermofluidynamic variables are presented in Tables 8 and 9. The convergence is reached in two iterations. An interesting fact that can be observed here is the absence of fouling in the final design, i.e. the proposed procedure was able to identify a “no fouling” solution. Based on this fact, the HTRI software provided a heat exchanger with an area 27% smaller. Additionally, the no fouling behavior would allow the continuous operation of the heat exchanger without the need of cleaning actions.

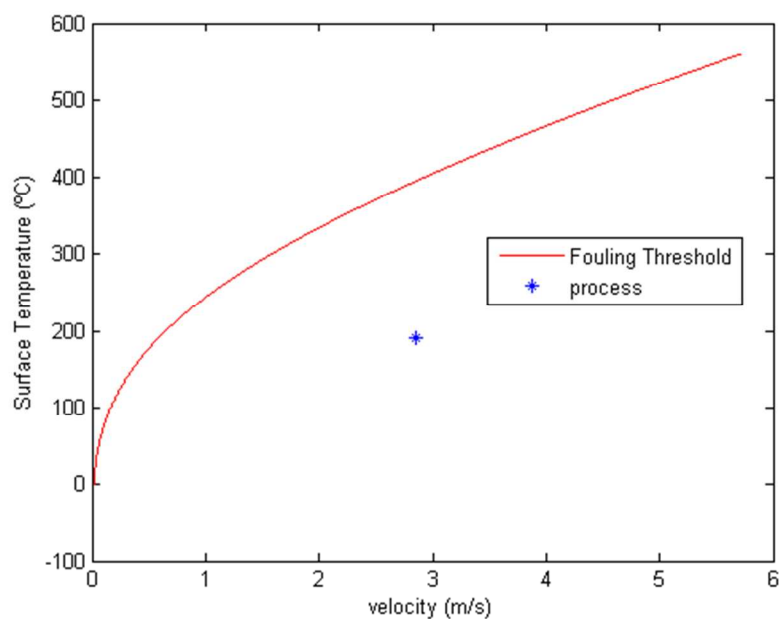
Table 8. Example 2 - Heat Exchanger Design Solutions: Design Variables

	initial design	final design
design fouling factor (m ² K/W)	0.000350	0
simulated fouling factor (m ² K/W)	0	0
area (m ²)	76.8	55.7
total number of tubes	235	235
number of tube passes	1	1
shell diameter (m)	0.438	0.438
tube length (m)	5.5	4.0
baffle spacing (m)	0.394	0.315

Table 9. Example 2 - Heat Exchanger Design Solutions: Thermofluidynamic Variables

	initial design	final design
overall heat transfer coefficient ($\text{W}/\text{m}^2\text{C}$)	660.7	955.9
tube-side film coefficient ($\text{W}/\text{m}^2\text{C}$)	2340.3	2367.2
shell-side film coefficient ($\text{W}/\text{m}^2\text{C}$)	2118.8	2172.0
tube-side flow velocity (m/s)	2.86	2.86
shell-side flow velocity (m/s)	0.96	1.12
tube-side pressure drop (kPa)	43.9	34.3
shell-side pressure drop (kPa)	66.0	65.4

The fouling envelope related to the threshold concept is illustrated in Figure 6, where it is possible to observe that the final design solution is inside the no fouling region.

**Figure 6.** Fouling envelope of Example 2

5.3. Example 3. The fouling rate model parameters are displayed in Table 8.

Table 8. Example 3 -Fouling Rate Model Parameters (Eq. (4))

	Parameter
α (m ² K/J)	7.36
E_a (kJ/mol)	65.5
γ (m ² K/J·Pa)	$4.17 \cdot 10^{-12}$

The proposed design procedure was applied considering three different campaigns between cleanings: 6 months, 2 years and 4 years. The corresponding solutions together with the initial heat exchanger designed using the TEMA fouling factor (initial design) are shown in Tables 9 and 10.

Table 9. Example 3 - Heat Exchanger Design Solutions: Design Variables

	initial design	6 months design	2 years design	4 years design
design fouling factor (m ² K/W)	0.00035	0.000236	0.000390	0.000424
simulated fouling factor (m ² K/W)	0.000424	0.000236	0.000390	0.000424
area (m ²)	76.8	69.7	76.8	83.8
total number of tubes	235	235	235	235
number of tube passes	1	1	1	1
shell diameter (m)	0.438	0.438	0.438	0.438
tube length (m)	5.5	5.0	5.5	6.0
baffle spacing (m)	0.393	0.426	0.393	0.440

Table 10. Example 3 - Heat Exchanger Design Solutions: Thermofluidynamic Variables

	initial design	6 months design	2 years design	4 years design
overall heat transfer coefficient (W/m ² °C)	660.7	726.8	638.6	617.20
tube-side film coefficient (W/m ² °C)	2340.5	2346.6	2338.4	2336.4
shell-side film coefficient (W/m ² °C)	2118.8	2073.0	2118.3	2075.1
tube-side flow velocity (m/s)	2.86	2.86	2.86	2.86
shell-side flow velocity (m/s)	0.96	0.90	0.96	0.88
tube-side pressure drop (kPa)	43.9	40.7	43.9	47.1
shell-side pressure drop (kPa)	66.0	53.2	66.0	61.1

1
2
3 The comparison of the results shows that the increase of the campaign duration implies in an
4 augmentation of the final fouling resistance in the solution. The design alternatives considering 2
5 years and 4 years of campaign present fouling resistances 65% and 80% higher than the 6
6 months design option, respectively. Consequently, the corresponding design solutions present
7 overall heat transfer coefficients 12% and 15% lower. This reduction of the overall heat transfer
8 coefficient determines an increase of the area with the duration of the campaign, where the
9 proposed procedure identifies solutions with crescent tube lengths.
10
11
12
13
14
15
16
17
18
19

20
21 This analysis indicates that the inclusion of the fouling rate model in the design procedure also
22 allows the investigation of a tradeoff involving capital costs and heat exchanger cleaning
23 schedule. The increase of the time span between cleanings reduces costs associated to the
24 maintenance activities and downtime, but demands higher capital costs.¹¹
25
26
27
28
29
30
31
32
33
34

35 6. CONCLUSIONS

36
37
38 Conventional heat exchanger design approaches involve the examination of different
39 alternatives towards feasible and cheaper solutions. During the search, all the solution candidates
40 present the same previously established fouling resistances, independently of the
41 thermofluidynamic variables, especially flow velocity and surface temperatures. However, this
42 approach contains a considerable level of inaccuracy, because different heat exchangers
43 proposed for the same service will present different levels of fouling.
44
45
46
47
48
49
50
51
52

53 The availability of fouling rate models that can predict the impact of the thermofluidynamic
54 conditions on fouling offers the opportunity, explored in the current paper, to propose more
55
56
57
58
59
60

1
2
3 effective design schemes for handling this problem. In this context, this paper presents a proposal
4
5 of interconnection between conventional design algorithms and fouling rate models. Therefore, it
6
7 is possible to insert the behavior of the fouling phenomenon during the design phase of the heat
8
9 exchanger, aiming its mitigation.
10
11

12
13
14 The resultant design scheme is explored using a commercial software for generating the design
15
16 and a computational routine for determination of the fouling resistance through the heat
17
18 exchanger dynamic simulation. The entire procedure is executed automatically. Computational
19
20 tests using the modified Ebert-Panchal model indicates that the proposal is able to modify the
21
22 design, exploring the predictions of the fouling rate. Considering the relevant economic losses
23
24 associated to fouling, the procedure may be a promise contribution for handling this problem at
25
26 design level. Further research may be devoted to include the design generation and the fouling
27
28 evaluation in a single optimization problem.
29
30
31
32
33
34
35
36

37 NOMENCLATURE

38
39
40 A = area (m^2)
41
42

43
44 C_p = heat capacity ($\text{J}/(\text{kg}\cdot\text{K})$)
45
46

47
48 C_{max} = heat capacity flow rate of the minimum fluid
49
50

51
52 C_{min} = heat capacity flow rate of the minimum fluid
53
54

55
56 C_R = ratio between heat capacity flow rates
57
58

59
60 d_{te} = outer tube diameter (m)

1
2
3 d_{ti} = inner tube diameter (m)
4
5

6
7 E_a = Activation energy (kJ/mol)
8
9

10 f = Fanning friction factor
11
12

13 h = convective heat transfer coefficient (W/(m²·K))
14
15

16
17 L = tube length (m)
18
19

20 k_{tube} = thermal conductivity of the tube wall (W/(m·K))
21
22

23
24 N_{pt} = number of tube passes
25
26

27 N_{tt} = total number of tubes
28
29

30 NTU = number of transfer units
31
32

33
34 Nu = Nusselt number
35
36

37 Pr = Prandtl number
38
39

40 Q = heat duty (W)
41
42

43
44 Q_{max} = maximum heat duty thermodynamically possible (W)
45
46

47 R = universal gas constant (J/(mol·K))
48
49

50
51 R_f = fouling factor (m²K/W)
52
53

54 Re = Reynolds number
55
56
57
58
59
60

1
2
3 $t =$ time (s)
4
5

6
7 $T =$ temperature ($^{\circ}\text{C}$)
8
9

10 $U =$ overall heat transfer coefficient ($\text{W}/(\text{m}^2\text{K})$)
11
12

13 $v =$ flow velocity (m/s)
14
15
16
17
18
19

20 **Greek letters**

21
22

23 $\alpha =$ Ebert and Panchal modified parameter ($\text{m}^2\text{K}/\text{J}$)
24
25

26
27 $\varepsilon =$ effectiveness
28
29

30 $\gamma =$ Ebert and Panchal modified parameter ($\text{m}^2\text{K}/\text{J}\cdot\text{Pa}$)
31
32
33

34 $\mu =$ dynamic viscosity ($\text{Pa}\cdot\text{s}$)
35
36

37 $\rho =$ specific mass (kg/m^3)
38
39

40
41 $\tau_w =$ wall shear stress (Pa)
42
43
44
45
46
47

48 **Subscripts**

49
50

51 $avg =$ average
52
53

54
55 $c =$ cold stream
56
57
58
59
60

1
2
3 *clean* =no fouled
4

5
6
7 *dirty* = design dirty condition
8

9
10 *foul* = fouled
11

12
13 *h* = hot stream
14

15
16
17 *i* = inlet
18

19
20 *max* = maximum fluid
21

22
23 *min* = minimum fluid
24

25
26
27 *o* = outlet
28

29
30 *s* = shell
31

32
33
34 *t* = tube
35
36
37
38
39

40 REFERENCES

41
42
43
44 (1) Bell, K. J. Logic of the design process. *Heat Exchanger Design Handbook*; Begell
45 House, 2008.
46

47
48
49 (2) Mizutani, F. T., Pessoa, F. L. P., Queiroz, E. M., Hauan, S., Grossmann, I. E.
50 Mathematical Programming Model for Heat-Exchanger Network Synthesis Including Detailed
51 Heat Exchanger Designs. 1, Shell-and-Tube Heat Exchanger Design, *Ind. Eng. Chem. Res.*,
52 **2003**, 42, 4009-4018.
53
54
55
56
57
58
59
60

1
2
3 (3) Ravagnani, M. A. S. S., Caballero, J. A. A MINLP model for the rigorous design of shell
4 and tube heat exchangers using the Tema standards. *Chem. Eng. Res. Des.*, **2007**, 85, 1423-1435.
5
6

7
8
9 (4) Gonçalves, C.O., Costa, A. L. H., Bagajewicz, M.J. Shell and tube heat exchanger design
10 using mixed-integer linear programming, submitted for publication, *AIChE J.*, **2016**.
11
12

13
14 (5) Ponce-Ortega, J. M., Serna-González, M., Jiménez-Gutiérrez, A. Use of genetic
15 algorithms for optimal design of shell-and-tube heat exchangers. *Appl. Therm. Eng.*, **2009**, 29,
16 203-209.
17
18
19

20
21 (6) Sadeghzadeh, H., Ehyaei, M. A., Rosen, M. A. Techno-economic optimization of a shell
22 and tube heat exchanger by genetic and particle swarm algorithms. *Energy Convers. Manager.*,
23 **2015**, 93, 84-91.
24
25
26
27

28
29 (7) Costa, A. L. H., Queiroz, E. M. Design optimization of shell-and-tube heat exchangers.
30 *Appl. Therm. Eng.*, **2008**, 28, 1798-1805.
31
32
33

34
35 (8) Butterworth, D. Design of shell-and tube heat exchangers when the fouling depends on
36 local temperature and velocity. *Appl. Therm. Eng.*, **2002**, 22, 789-801.
37
38
39

40
41 (9) Wilson, D. I., Polley, G. T., Pugh, S. J. Mitigation of crude oil preheat train fouling by
42 design. *Heat Transfer Eng.*, **2002**, 23, 24-37.
43
44
45

46
47 (10) Nesta, J., Bennet, C.A. Reduce fouling in shell-and-tube heat exchangers, *Hydrocarbon*
48 *Process.*, **2004**, 83, 77 -82.
49
50

51
52 (11) Caputo, A. C., Pelagagge, P. M., Salini, P. Joint economic optimization of heat exchanger
53 design and maintenance policy. *Appl. Therm. Eng.*, **2011**, 31, 1381-1392.
54
55
56
57
58
59
60

1
2
3 (12) Müller-Steinhagen, H. Heat Transfer Fouling: 50 Years After the Kern and Seaton
4 Model. *Heat Transfer Eng.*, **2011**, 32, 1-13.
5
6

7
8
9 (13) Wilson, D. I., Ishiyama, E. M., Polley, G. T. Twenty years of Ebert and Panchal - What
10 next?, *Heat Exchanger Fouling and Cleaning Conference*, Dublin, Ireland, 2015.
11
12

13
14 (14) Ebert, W., Panchal, C. B. Analysis of Exxon crude oil slip stream coking data, *Fouling*
15 *Mitigation of Industrial Heat-Exchange Equipment*, San Luis Obispo, USA, 1995.
16
17

18
19
20 (15) Wilson, D. I., Polley, G. T., Pugh, S. J. Ten years of Ebert, Panchal and the “threshold
21 fouling” concept, *Heat Exchanger Fouling and Cleaning Conference*, KlosterIrsee, Germany,
22 2005.
23
24
25

26
27
28 (16) Panchal, C. B., Kuru, W. C., Liao, C. F., Ebert, W. A., Palen, J. W. Threshold conditions
29 of crude oil fouling, *Understanding Heat Exchanger Fouling and Mitigation*, Begell House,
30 1999.
31
32
33

34
35
36 (17) Polley, G. T., Wilson, D. I., Yeap, B. L., Pugh, S. J., Evaluation of laboratory crude oil
37 threshold fouling data for application to refinery pre-heat trains. *Appl. Therm. Eng.*, **2002**, 22,
38 777-788.
39
40
41

42
43
44 (18) Nasr, M. R. J., Givi, M. M. Modeling of crude oil fouling in preheat exchangers of
45 refinery distillation units, *Appl. Therm. Eng.*, **2006**, 26, 1572-1577.
46
47
48

49
50 (19) Lestina, T. G., Zettler, H. U., Crude Oil Fouling Research: HTRI's Perspective, *Heat*
51 *Transfer Eng.*, **2014**, 35, 217-223.
52
53
54

1
2
3 (20) Saunders, E. A. D., *Heat Exchangers: Selection, Design & Construction*, Longman
4
5 Scientific & Technical, 1988.
6
7

8
9 (21) Diaz-Bejarano, E., Coletti, F., Macchietto, S. Crude oil fouling deposition, suppression,
10 removal – and how to tell the difference, *Heat Exchanger Fouling and Cleaning Conference*,
11 *Dublin*, Ireland, 2015.
12
13
14

15
16
17 (22) Ishiyama, E. M., Paterson, W. R., Wilson, D. I., Thermo-hydraulic channeling in parallel
18 heat exchangers subject to fouling, *Chem. Eng. Sci.*, **2008**, 63, 3400-3410.
19
20
21

22
23 (23) Incropera, F. P., DeWitt, D. P. *Fundamentals of Heat and Mass Transfer*, John Wiley &
24 Sons, 2006.
25
26
27

28 (24) TEMA, *Standards of the Tubular Exchanger Manufacturers Association*, 9th Edition,
29 2007.
30
31
32
33
34
35
36
37
38
39
40
41
42
43
44
45
46
47
48
49
50
51
52
53
54
55
56
57
58
59
60



Figure 1.Representation of the threshold concept in relation to the surface temperature (T_{surf}) and the flow velocity (v).

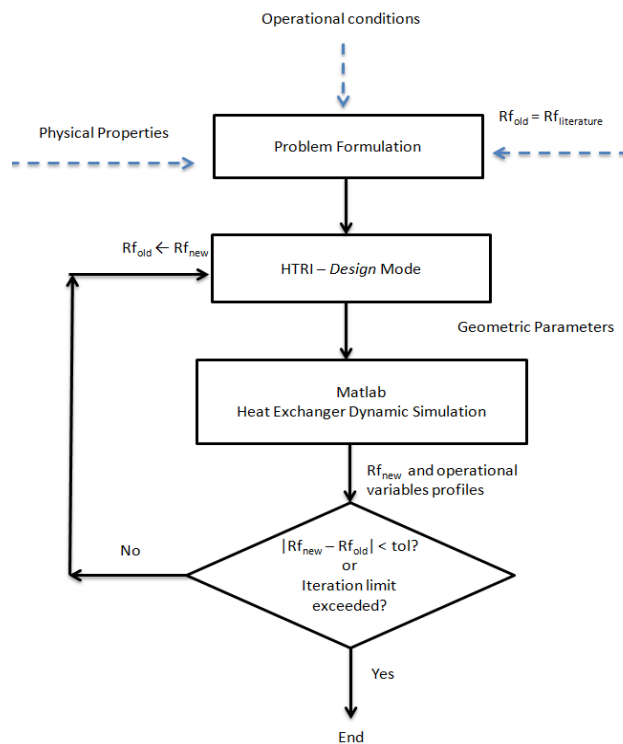


Figure 2. Design procedure using fouling rate modelling.

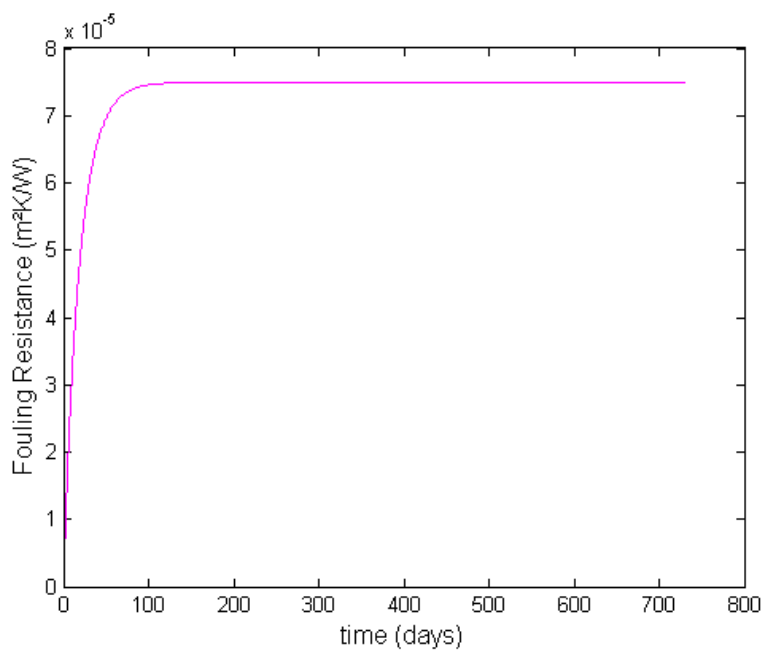


Figure 3. Fouling resistance profile of Example 1

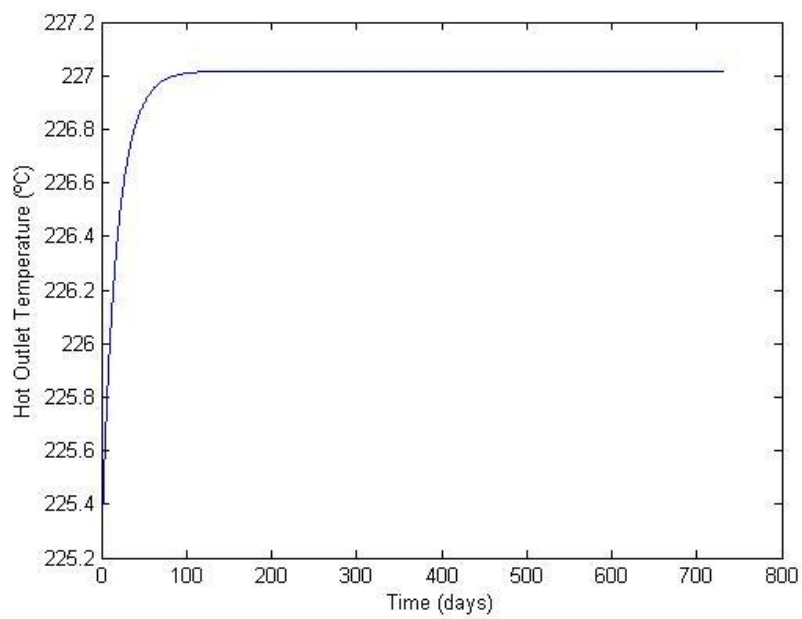


Figure 4. Outlet temperature of the hot stream in Example 1

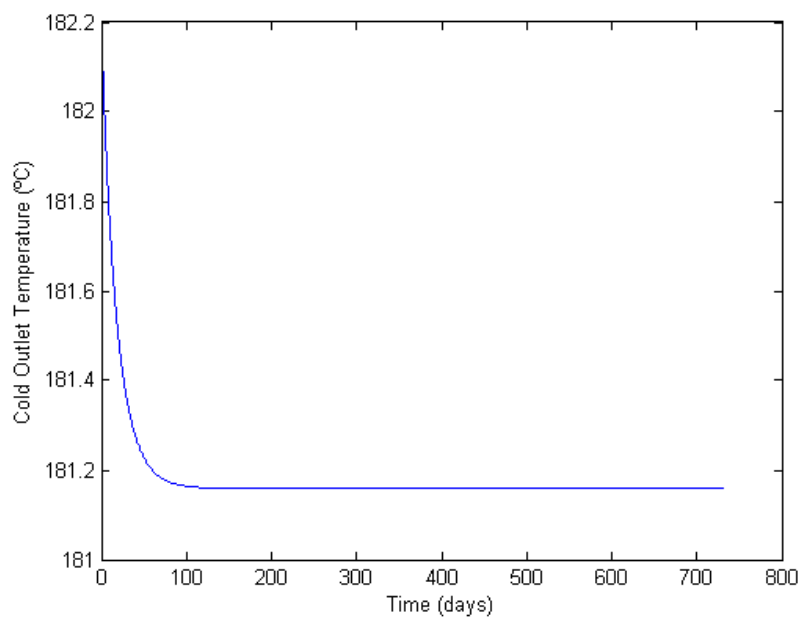


Figure 5. Outlet temperature of the cold stream in Example 1

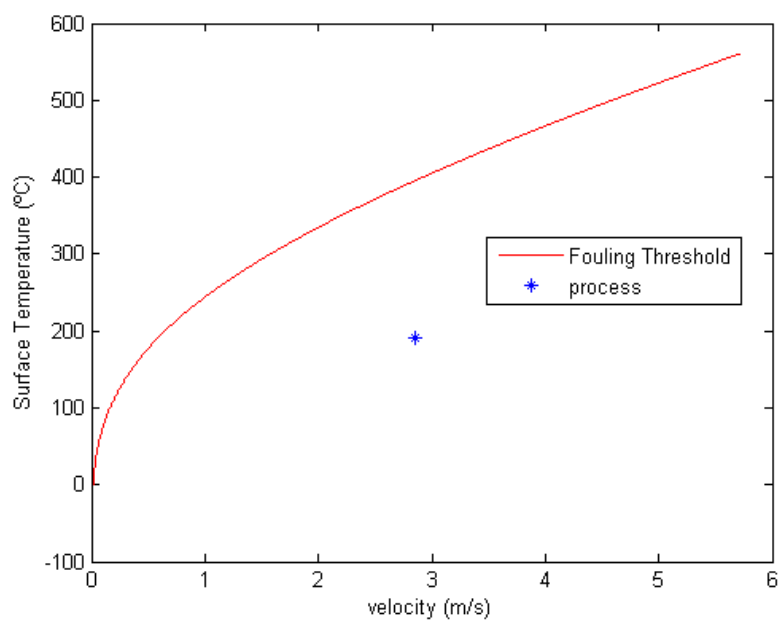


Figure 6. Fouling envelope of Example 2